Asian Journal of Chemistry; Vol. 36, No. 8 (2024), 1781-1792

ASIAN JOURNAL OF CHEMISTRY

https://doi.org/10.14233/ajchem.2024.31669

# Co(II), Ni(II), Cu(II) and Zn(II) Metal Complexes of Hydrazone Schiff Base Ligand: Synthesis, Characterization, Thermal Behaviour, Antioxidant and Antimicrobial Studies

TUSHAR S. UMASARE*, SANJAY K. PATIL and JYOTSNA G. PARGAONKAR

Department of Chemistry, Changu Kana Thakur Arts, Commerce and Science College, New Panvel-Raigad, Navi Mumbai-410206, India

*Corresponding author: Tel: +91 22 27464193/27455760; E-mail: tusharumasare87@gmail.com

*Received*: 5 April 2024; *Accepted*: 22 May 2024; *Published online*: 25 July 2024; AJC-21699

The metal(II) complexes of ML type of Co(II), Ni(II), Cu(II) and Zn(II) were synthesized using hydrazone Schiff base, *N*′,*N*′′-((1*E*,2*E*)-acenaphthylene-1,2-diylidene)*bis*(2-hydroxy benzohydrazide), which was synthesized by the condensation of acenaphthaquinone and 2-hydroxy benzohydrazide (1:2 molar ratio) in ethanol and characterized by various spectroscopic and analytical techniques, including UV-visible, FTIR, $^{1}$H NMR, $^{13}$C NMR, LC-MS, TGA-DSC, powder XRD and atomic absorption measurements. The magnetic susceptibility and electronic spectral data suggested that the Ni(II) and Cu(II) complexes have octahedral geometry, while the Co(II) and Zn(II) complexes have tetrahedral geometry. It has also been found that all the metal(II) complexes are paramagnetic, except Zn(II) complex. The molar conductance values indicated that all the metal(II) complexes are non-electrolytes in DMSO solvent. The stability of metal(II) complexes, the absence of coordinated and lattice water molecules in complexes and the proposed formula were all validated by the thermal analysis. All the compounds have average crystallite sizes on the nanoscale, according to powder XRD results. All of the compounds were tested for their *in vitro* antimicrobial activities against six bacteria (*B. subtilis*, *S. aureus*, *Corynebacterium*, *P. aeruginosa*, *K. pneumoniae* and *E. coli*) and three fungi (*C. albicans*, *A. flavus* and *A. niger*) at two different concentrations.

**Keywords: Hydrazone Schiff base, Metal(II) complexes, Acenaphthaquinone, 2-Hydroxy benzohydrazide, Biological activities.**

## INTRODUCTION

The hydrazones containing (-C=N-NH-CO-) groups, a unique class of Schiff bases, have been the subject of much research due to their physiological and biological activities, applicability in analytical chemistry and coordination ability [1-3]. They exhibit keto-enol tautomerism, which provides molecules an additional donor site and coordinate in neutral or anionic mode with metal ions through the imine-N atom and the amide oxygen atom (protonated/deprotonated form), resulting in the formation of mononuclear or binuclear complexes [4,5]. However, they depend on reaction parameters such as the pH of the medium, the structure of hydrazone, nature of the solvent and metal ions [6].

A large number of metal ion complexes have been reported with hydrazone Schiff bases, possessing antibacterial, antifungal [7-9], antioxidant [10], antitumor [11,12], antidepressant [13], analgesic, anti-inflammatory [14,15], antitubercular [16,17], anticonvulsant [18], antimalarial [19], antihypertensive [20], DNA-binding [21,22] and sensor [23,24] properties. They also act as active insecticidal, nematicidal and herbicidal agents and plant growth regulators [25,26]. For example, Cu(II) and Zn(II) complexes derived from the hydrazone Schiff base ligand exhibited cytotoxicity activity against HeLa and U937 cancer cell lines [27]. Hydrazones of salicylic acid derivatives complexed with Co(II), Cu(II) and Ni(II) have considerable inhibitory and urease activity [28]. Furthermore, specific acenaphthaquinone derivatives exhibit a diverse range of biological characteristics [29-31]. For instance, Zn(II) complex of acenaphthene benzohydrazide-based ligand had certain photoluminescence and fluorescence properties [32]. Additionally, the complexes of Co(II), Ni(II), Cu(II) and Zn(II) with the $N_2O_2$ ligand acenaphthacene showed DNA intercalating binding properties [33].

Specific transition metal complexes of Schiff base derived from acenaphthenequinone and essential amino acids [34] have been found to possess DNA breakage ability and antibacterial activity. The Schiff bases derived from acenaphthaquinone and their metal(II) complexes have shown considerable antimicrobial properties [35-37]. Considering the significance linked to hydrazones, herein, the synthesis and characterization of

novel hydrazone Schiff base, *N*′,*N*′′-((1*E*,2*E*)-acenaphthylene-1,2-diylidene)*bis*(2-hydroxy benzohydrazide) (HBH-ANQ) and its metal complexes with Co(II), Ni(II), Cu(II) and Zn(II) ions are carried out. The antioxidant and antimicrobial activities of both novel ligand and its metal(II) complexes were also assessed.

## EXPERIMENTAL

The required chemicals were purchased from several reliable commercial suppliers and used as supplied. A Shimadzu UV-160 spectrophotometer was used to record the electronic spectra in DMSO solvent. Using an Elico CM 180 conductivity meter, molar conductance was measured in DMSO solution at concentrations of $10^{-3}$ M. The magnetic moment was measured by the Gouy method using the Digital Gouy Balance GMX-02 model. Using KBr pellet, the Shimadzu FTIR model 4800S spectrophotometer captured the infrared spectra within the 4000-400 $cm^{-1}$ range. The $^1H$ & $^{13}C$ NMR spectra of Schiff base were measured in DMSO-$d_6$ solvent with TMS as an internal standard on Bruker Advance III 400 MHz and 100 MHz spectrophotometers, respectively. The mass range of 20000 amu in ToF was used to record mass spectra using LC-MS. The microanalyses for the elements C, H and N were recorded using a CHNS microanalyzer. The Shimadzu atomic absorption 160 spectrophotometer was used to measure the amount of metal present in the complexes. Using Cu*K*α1 radiation (λ = 1.54060 Å) at 40 kV and 40 mA, powder XRD patterns were obtained in the range of 5º-70º 2θ values on the Ultima IV X-ray diffractometer. The Perkin-Elmer simultaneous thermal analyzer (STA-6000) device was used to obtain the thermogravimetric curves of all the metal(II) complexes in $N_2$ environment, with a heating rate of 20 ºC/min and a temperature range of 50-800 ºC.

**Synthesis of 2-hydroxybenzohydrazide:** In an ice-cooled ethanolic solution (25 mL) of methyl salicylate (7.60 g, 6.4 mL, 50 mmol), hydrazine hydrate (5.0 g, 100 mmol) was added gradually while stirring continuously over the period of 30 min. This reaction mixture was refluxed for about 5 h, then concentrated and cooled. On cooling, the white solid separated was filtered and washed with a minimum quantity of ethanol. This crude solid was recrystallized from ethanol and finally dried over anhydrous $CaCl_2$ in a vacuum desiccator. The reaction was monitored by TLC technique using the solvent system, diethyl ether: *n*-hexane (1:1 v/v) (**Scheme-I**, step-1) [38]. White solid, yield: 86%, m.p.: 142-144 ºC, IR (KBr, $\nu_{max}$, $cm^{-1}$): 3319, 3271 (N-H); 3055, 3010 (C-H aromatic), 1647 (C=O), 1529 (C=C), 1238 (C-O).

**Synthesis of Schiff base ligand, *N*′,*N*′′-((1*E*,2*E*)-acenaphthylene-1,2-diylidene)*bis*(2-hydroxy benzohydrazide), (HBH-ANQ):** A warm ethanolic solution of acenaphthoquinone (3.64 g, 20 mmol) was added slowly portionwise to hot ethanolic (30 mL) solution of 2-hydroxy benzohydrazide (6.08 g, 40 mmol) with constant stirring and then heated the reaction mixture for 4 h under reflux condition. The reaction process was monitored using the TLC technique with a solvent system consisting of *o*-xylene:acetone (60:40 v/v). The resulting solution was concentrated to one-half by distilling out the solvent under reduced pressure and allowed to cool to room temperature. The bright yellow solid formed, separated by filtration and subse-

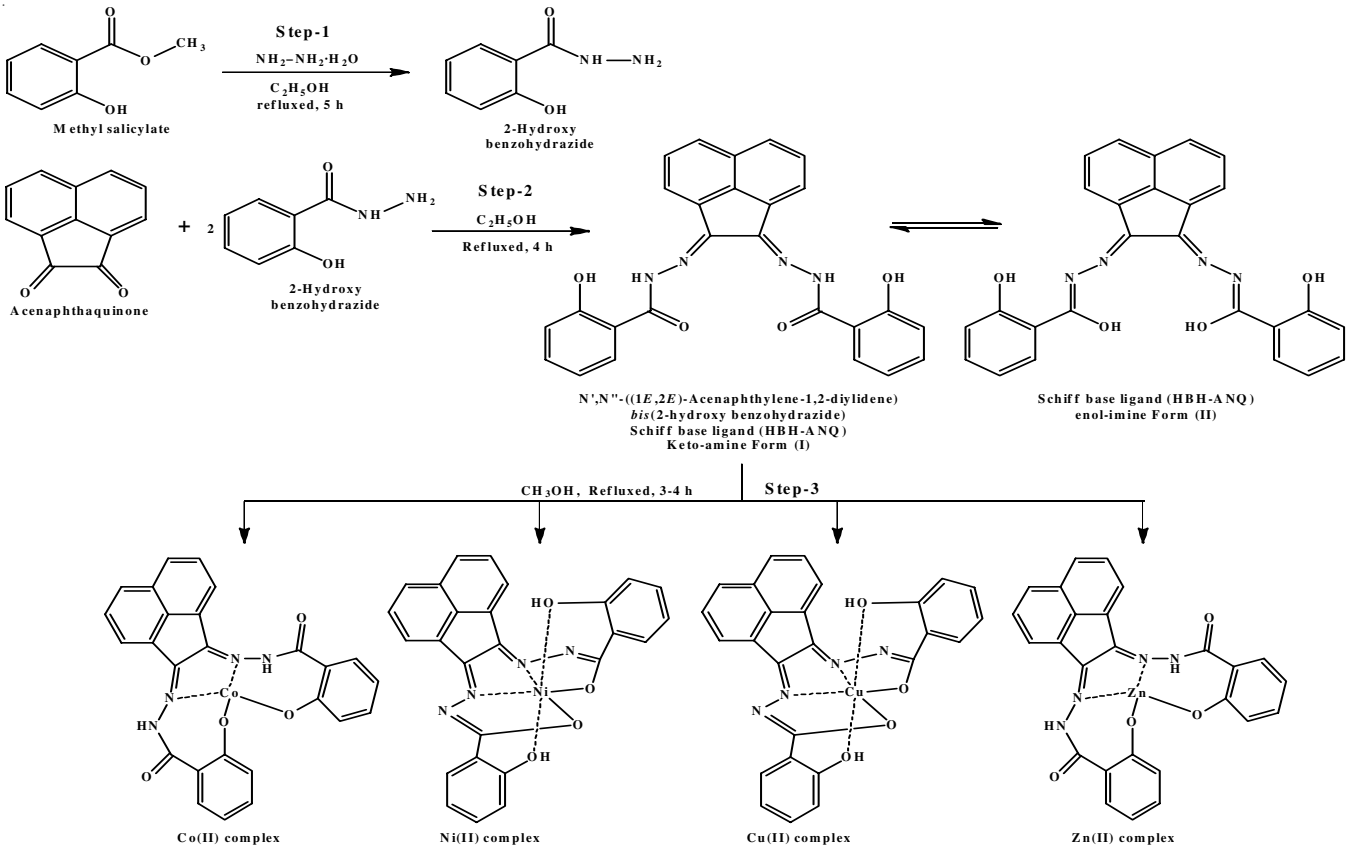


**Scheme-I:** Synthetic route of Schiff base ligand (HBH-ANQ) and its metal complexes

quently rinsed multiple times using a minimal quantity of ethanol followed by chloroform. The resulting product was dried overnight over anhydrous $CaCl_2$ in a vacuum desiccator. The purity of the product was also assessed on a TLC plate using the identical solvent system (**Scheme-I**, step 2). $^1$H NMR (400 MHz, DMSO-$d_6$) δ ppm: 14.42 (s, 1H), 12.17 (s, 2H), 8.59 (d, *J* = 6.8 Hz, Ar-1H), 8.16 (dd, *J* = 7.2 Hz,6.8 Hz, Ar-2H), 7.95 (s, N-H,1H), 7.83-7.95 (m, Ar -3H), 7.57-7.66 (m, Ar-2H), 7.35-7.42 (m, Ar-2H), 7.02 (d, *J* = 5·6Hz, Ar-2H), 6.87 (dd, *J* = 7.2 Hz,8.0 Hz, Ar-2H); $^{13}$C NMR (100 MHz, DMSO) δ ppm: 167.4, 161.8, 159.4, 156.4, 147.1, 145.2, 134.7, 132.7, 131.9, 130.6, 129.7, 129.1, 128.4, 127.6, 127.5, 122.7, 120.5, 119.8, 119.1, 117.3.

**Synthesis of Co(II), Ni(II), Cu(II) and Zn(II) metal complexes:** Solid Co(II), Ni(II), Cu(II) and Zn(II) complexes of Schiff base ligand (HBH-ANQ) were synthesized using the following general procedure, involving the use of metal salts such as $CoCl_2{\cdot}6H_2O$, $NiCl_2{\cdot}6H_2O$, $CuCl_2{\cdot}2H_2O$ and $ZnCl_2$. To a hot methanolic solution (about 50-60 mL) of Schiff base (4.5 g, 10 mmol), about 12-15 mL methanolic solution of metal(II) chloride salt (10 mmol) was added gradually with constant stirring. This metal-Schiff base mixture was further refluxed for 3-5 h at a temperature of approximately 65 ºC to accomplish full complexation. After the refluxation, one-half of the volume of the resultant solution was removed *via* distillation under reduced pressure. After being cooled overnight at room temperature, the solid metal(II) complexes were isolated, filtered and washed repeatedly with methanol and diethyl ether. The obtained products dried overnight over anhydrous $CaCl_2$ in vacuum desiccators (**Scheme-I**, step 3).

### Biological study

**Antioxidant screening:** The antioxidant activities of free ligand and its metal(II) complexes were conducted using a 2,2-diphenyl-1-picrylhydrazyl (DPPH) assay, as this free radical scavenging assay is a rapid and reliable method for determining the radical scavenging activity of potential antioxidants [39]. Stock solutions of the test compounds were prepared using DMSO solvent. Various amounts of the test compounds with different concentrations (100-500 µg/mL) were diluted with ethanol and subsequently added to an ethanol solution containing DPPH. A combination of DPPH solution and ethanol served as a control, while ascorbic acid is the standard drug. After vigorous shaking, the resulting mixtures were incubated at room temperature for 30 min in dark. The absorbance at 517 nm was measured using a UV-Vis spectrophotometer to ascertain the radical scavenging capacity of an antioxidant activity [40]. The DPPH free radical scavenging activity was calculated by using the following equation:

$$\text{DPPH scavenging activity } (\%) = \frac{A_{control} - A_{test}}{A_{control}} \times 100$$

**Antimicrobial screening:** The antimicrobial activity of Schiff base ligand (HBH-ANQ) and its metal(II) complexes against three Gram-positive bacteria (*Staphylococcus aureus Bacillus subtilis* and *Corynebacterium*), three Gram-negative bacteria (*Pseudomonas aeruginosa*, *Klebsiella pneumoniae* and *Escherichia coli*) and three fungi (*Candida albicans*, *Aspergillus flavus* and *Aspergillus niger*) was evaluated *in vitro* using the disc diffusion method. This approach used Sabouraud dextrose agar and Muller-Hinton agar as growth media for fungi and bacteria, respectively. The sterile agar medium was prepared according to the the directions provided by the manufacturer and then aseptically transferred to sterilized Petri plates in the required volume and were then left to harden. A 100 µL of bacterial/fungi under investigation were grown in 10 mL of fresh media until they reached the appropriate count of microorganisms. For inoculation, 100 µL of fresh microbial suspension was applied on the surface of each agar plate spread evenly over the medium and allowed to set. Stock sample solutions were obtained by dissolving the tested compounds in DMSO solvent. Test sample DMSO solutions of known concentration were put onto blank sterile discs to produce 50 and 100 µg of test sample per disc. The impregnated sample discs were positioned carefully at equal distances and gently pressed down on inoculated agar plates. The plates were incubated for 24-48 h at 35-37 ºC for bacteria and 24-48 h at 25-27 ºC for fungus, respectively. Blank sterile discs soaked in DMSO were employed as a negative control and readymade discs of standard drugs (ciprofloxacin for bacteria and fluconozole for fungi) served as positive controls for the antimicrobial activity. During the incubation time, the test solution diffused and affected the proliferation of microorganisms, resulting in the development of an inhibitory zone. The diameter of the inhibitory zone surrounding each disc (in mm) was measured [35,41].

## RESULTS AND DISCUSSION

The structure of novel Schiff base was elucidated by several analytical and physical techniques. The metal(II) complexes were formed using the synthesized hydrazone Schiff base in equimolar ratio. The obtained analytical and physical results were in good agreement with the suggested composition of hydrazone Schiff base and its metal(II) complexes (Table-1). The synthesized metal(II) complexes are coloured, stable in air and insoluble in water, but completely soluble in dimethyl sulfoxide (DMSO) and dimethyl formamide (DMF) solvents. The molar conductance of the metal(II) complexes in DMSO at a concentration of $10^{-3}$ M, varied from 3 to 18 $cm^2$ $Ohm^{-1}$ $mol^{-1}$ at room temperature, suggesting that they are non-electrolytic in nature [42].

**NMR spectral studies:** The $^1$H NMR spectrum of the novel hydrazone Schiff base (HBH-ANQ) recorded in DMSO displayed a downfield singlet at δ 14.42 ppm and one overlapped signal at δ 7.95 ppm. These signals can be ascribed to the enolic proton (-N=C-O**H**) and the amide proton (-N**H**-C=O) of the hydrazone moiety, respectively, each integrating for one proton. This suggests that the ligand is in the keto-enol tautomeric form (**Scheme-I**) in solution state (in DMSO) [3,5,42]. Intramolecular hydrogen bonding may exist because of the signal that appears at δ 12.17 ppm, downfield from TMS and is attributed to the proton nucleus of phenolic (O-H) groups [43]. In the aromatic region δ (6.86-8.60) ppm, a set of peaks were detected, which corresponded to the 14 aromatic protons of the benzene and acenaphthene rings [32].

TABLE-1
PHYSICAL AND ANALYTICAL DATA OF SCHIFF BASE (HBH-ANQ) AND ITS METAL COMPLEXES

| Compounds (m.f.) | m.w. (g mol$^{-1}$) | Colour | m.p. (°C) | Yield (%) | Elemental analysis (%): Found (calcd.) | | | | $\Lambda_m$ (cm$^2$ $\Omega^{-1}$ mol$^{-1}$) in DMSO |
|---|---|---|---|---|---|---|---|---|---|
| | | | | | C | H | N | M | |
| HBH-ANQ ($C_{26}H_{18}N_4O_4$) | 450.45 | Bright yellow | > 300 | 82 | 69.63 (69.32) | 4.08 (4.03) | 12.48 (12.44) | – | 0 |
| [Co(HBH-ANQ)] (Co $C_{26}H_{16}N_4O_4$) | 507.36 | Greenish yellow | > 300 | 74 | 61.22 (61.54) | 3.25 (3.17) | 10.91 (11.04) | 11.92 (12.87) | 12 |
| [Ni(HBH-ANQ)] (Ni $C_{26}H_{16}N_4O_4$) | 507.12 | Bright red | > 300 | 85 | 61.27 (61.58) | 3.28 (3.18) | 10.92 (11.04) | 10.95 (11.57) | 18 |
| [Cu(HBH-ANQ)] (Cu $C_{26}H_{16}N_4O_4$) | 511.98 | Brick red | > 300 | 82 | 62.63 (62.00) | 3.36 (3.15) | 11.17 (10.94) | 11.90 (12.41) | 06 |
| [Zn(HBH-ANQ)] (Zn $C_{26}H_{16}N_4O_4$) | 513.81 | Pale yellow | > 300 | 77 | 60.78 (60.52) | 3.24 (3.14) | 10.81 (10.90) | 12.06 (12.72) | 03 |

In $^{13}$C NMR spectrum, the Schiff base ligand showed signals at δ 156.49 and δ 167.49 ppm assigned to azomethine carbon (-C=N-) and amide carbonyl carbon (C=O) of the ligand, respectively [10,32]. Moreover, the absence of the ketonic carbonyl carbon (C=O) signal of acenaphthoquinone, which resonates near at δ 185 ppm, suggests that both carbonyl groups of acenaphthoquinone were consumed in the formation of the product. The ligand displays keto-enol tautomerism, as evidenced by the enolic carbon (-N=**C**-OH) signal found at δ 159.43 ppm. The signals associated with aromatic carbon atoms in acenaphthene and benzene rings were detected at δ 117-147 ppm [32,44].

**Mass spectral studies:** To validate the suggested structural formulas, the TOF ES mass spectra of free Schiff base and its corresponding metal(II) complexes were recorded at room temperature. The molecular ion peaks in the mass spectrum (Fig. 1) of Schiff base (HBH-ANQ) observed as $[M+H]^+$ at *m/z* 451.16 (94.1%), $[M+Na]^+$ at *m/z* 473.15 (45.7%) and $[2M+Na]^+$ at *m/z* 923.30 (15%). These values are in good agreement with the proposed molecular formula $[C_{26}H_{18}N_4O_4]$, which has an estimated molecular weight of 450.45 g/mol. The proposed fragmentation pattern, illustrated in **Scheme-II**, suggests that there are three possible pathways for fragmentation. The base peak at *m/z* = 301.16 (100%) corresponds to the fragments $[C_{19}H_{15}N_3O]^+$ or $[C_{19}H_{13}N_2O_2]^+$, which may result from the removal of $(C_7H_3NO_3)$ group in Route-1 or the removal of the $(C_7H_5N_2O_2)$ group in Route-2, respectively. The other fragments of the compound provide the distinctive peaks with varying intensities at different *m/z* values at 359 $[(C_{20}H_{13}N_4O_3)+2H]^+$, 338 $[(C_{20}H_{11}N_4O_2)-H]^+$, 331 $[(C_{19}H_{14}N_4O_2)+H]^+$, 317 $[C_{19}H_{15}N_3O_2]^+$, 313 $[C_{19}H_{13}N_4O]^+$, 284 $[C_{19}H_{12}N_2O]^+$, 247 $[C_{14}H_7N_4O]^+$, 229 $[(C_{14}H_6N_4)-H]^+$, 205 $[C_{13}H_7N_3]^+$, 199 $[(C_{12}H_{11}N_3)+2H]^+$, 183 $[(C_{12}H_{10}N_2)+H]^+$, 180 $[C_{12}H_8N_2]^+$, 149 $[(C_7H_6N_2O_2)-H]^+$, 141 $[C_{11}H_9]^+$, 126 $[C_{10}H_6]^+$, 121 $[C_7H_5O_2]^+$, 104 $[C_7H_4O]^+$, 93 $[C_6H_5O]^+$ and 77 $[C_6H_5]^+$ and validates the formation of the Schiff base structure.

The most significant peak in the mass spectra of the Co(II), Ni(II), Cu(II) and Zn(II) complexes of Schiff base (HBH-ANQ) was the molecular ion peak, which was observed at *m/z* 507.32, 507.08, 512.16 and 513.52, respectively and aligned with the suggested formulae of the complexes. The data acquired from CHN analyses and spectrum analyses of all metal complexes

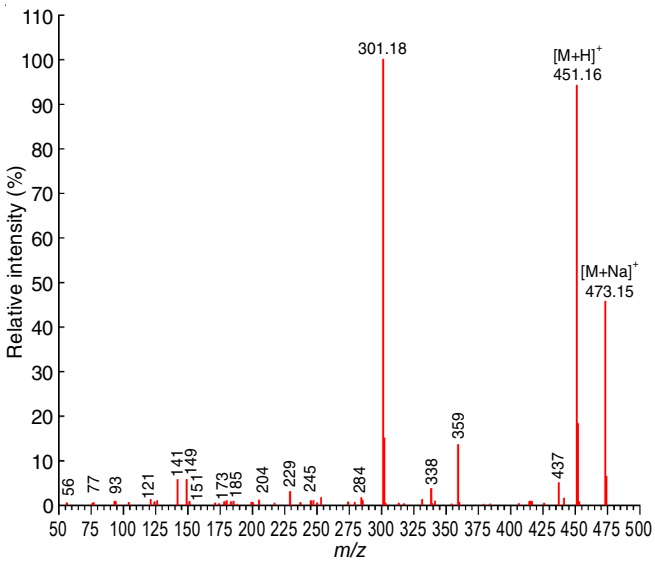


Fig. 1. Mass spectrum of Schiff base ligand (HBH-ANQ)

are consistent with the experimental mass spectral data, indicating that the metal complexes belong to the [ML] type.

**FTIR spectral studies:** The binding site of the ligand in metal(II) complexes can be determined a lot by comparing the infrared spectra of the free ligand and its metal(II) complexes. Table-2 lists the selected IR vibrations and approximate assign-

TABLE-2
SELECTED FT-IR STRETCHING FREQUENCY OF LIGAND (HBH-ANQ) AND ITS METAL COMPLEXES (cm$^{-1}$)

| Assignment | Ligand | Complexes of Schiff base ligand | | | |
|---|---|---|---|---|---|
| | | Co(II) | Ni(II) | Cu(II) | Zn(II) |
| $\nu$(O-H)$_{phenolic}$ | 3338 | – | 3406 | 3397 | – |
| $\nu$(N-H) | 3209 | 3215 | – | – | 3209 |
| $\nu$(C-H)$_{Arom.}$ | 3157 | 3157 | 3065 | 3064 | 3159 |
| | 3052 | 3050 | 3012 | 3022 | 3053 |
| $\nu$(C=O) | 1642 | 1643 | – | – | 1643 |
| $\nu$(C=N) | 1594 | 1568 | 1569 | 1572 | 1566 |
| $\nu$(C-O)$_{enolic}$ | – | – | 1421 | 1420 | – |
| $\nu$(N-N) | 1108 | 1120 | 1131 | 1129 | 1118 |
| $\nu$(M-O) | – | 572 | 568 | 565 | 561 |
| | – | – | 536 | 532 | – |
| $\nu$(M-N) | – | 483 | 482 | 458 | 480 |

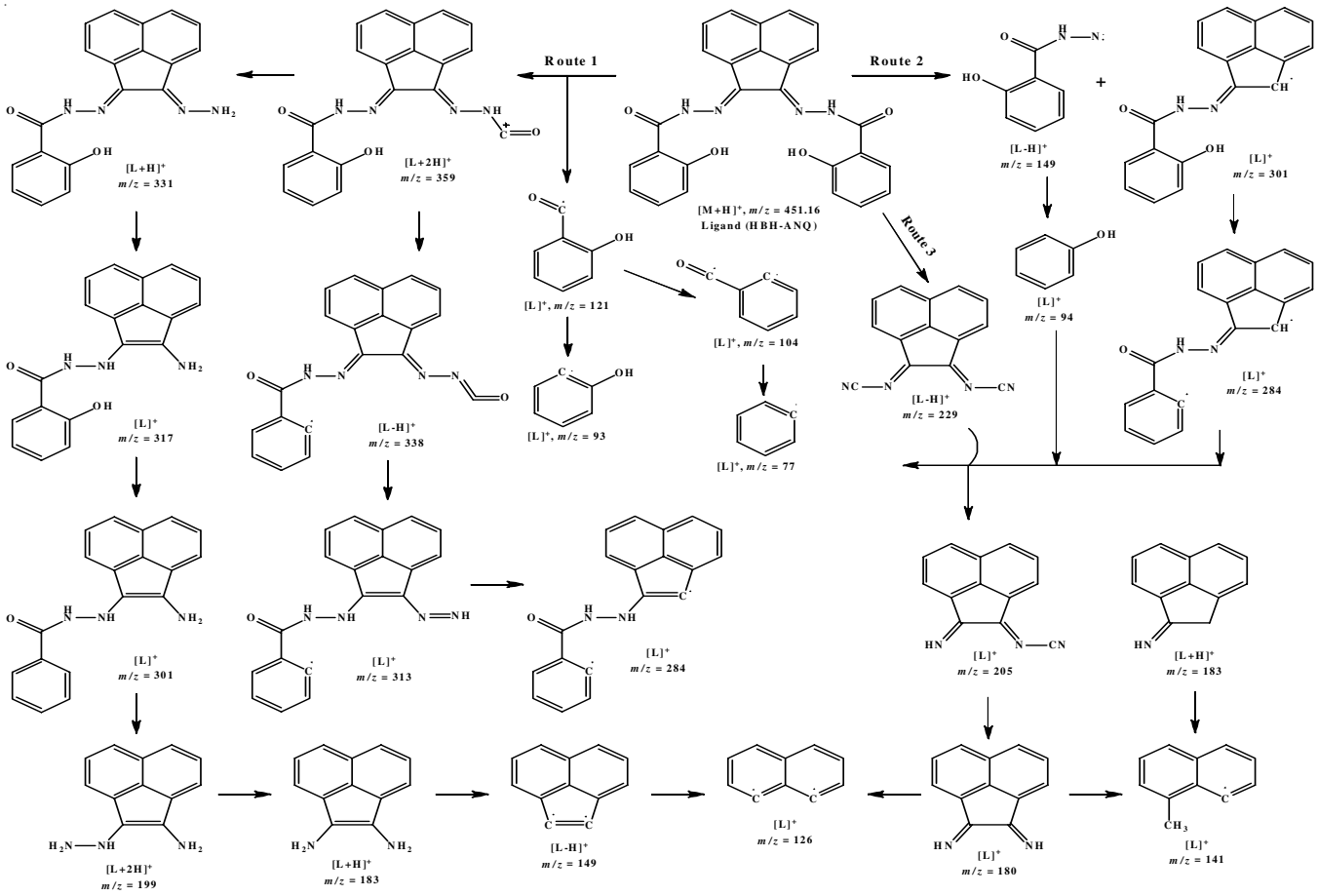


**Scheme-II:** Praposed mass fragmentation pathways of Schiff base ligand (HBH-ANQ)

ments for the ligand (HBH-ANQ) and its metal(II) complexes. The infrared spectra of Schiff base (HBH-ANQ) (Fig. 2) showed a prominent absorption band at 3338 $cm^{-1}$ and a shoulder at 3209 $cm^{-1}$, which were attributed to the stretching vibrations of ν(O-H) and ν(N-H), respectively. Also, the absorption bands at 3157 and 3052 $cm^{-1}$corresponded to the stretching vibrations of aromatic (C-H). Azomethine group ν(C=N) and amide carbonyl group stretching vibrations are responsible for the strong peaks at 1594 and 1642 $cm^{-1}$, respectively. Strong bands at 1510 and 1484 $cm^{-1}$ are caused by the acenaphthene ring conjugating with an exocyclic >C=N- group. This shows that ligand exists in the solid state in the form of keto-amine [32,43,45].

In the infrared spectrum of [Ni(HBH-ANQ)] and [Cu(HBH-ANQ)] complexes, the ligand band attributed to the exocyclic ν(C=N) azomethine group shifted to a lower wavenumber. This shift was observed at 1569 $cm^{-1}$ and 1572 $cm^{-1}$, respectively. The shift indicates that the azomethine-N is involved in coordination with the respective metal ion. This is supported by the displacement of the ν(N-N) peak, which initially appeared at 1108 $cm^{-1}$ in free ligand towards higher frequency in the complexes [4]. The absence of ligand bands for ν(N-H) and ν(C=O) and an appearance of new moderately intense bands at 1555-1520 and 1554-1525 $cm^{-1}$ in the Ni(II) and Cu(II) complexes, respectively, are indicative of the (-C=N-N=C-) stretching-bending vibrations. These vibrations suggest that the ligand experienced the enolization and deprotonation of the (N-H) group over the formation of the complex. In addition, new absorption bands at 1421-1287 and 1420-1278 $cm^{-1}$ were ascribed to the stretching of enolic (C-O) and the five-membered chelate ring formed as the enolic-O and azomethine-N coordinated with metal ion in the Ni(II) and Cu(II) complexes, respectively. The assertion was supported by missing of the prominent ligand band at 1539 $cm^{-1}$ in the spectrum of both complexes, which was indicative of C–N–H stretch-bend vibrations for a non-cyclic monosubstituted amide. The appearance of a new band at 1252-1251 $cm^{-1}$, which could be due to the coupled chelate ring, C-OH and phenyl ring stretching vibrations and the upward shift of the phenolic (O-H) stretching and bending bands of the ligand from 3338-1348 $cm^{-1}$ to 3406-1382 and 3397-1360 $cm^{-1}$ in the Ni(II) and Cu(II) complexes, respectively, suggest that the phenolic (OH) group of the ligand is involved in the coordination of metal ions. The absorption bands observed at 568 $cm^{-1}$, 536 $cm^{-1}$, 482 $cm^{-1}$ and 565 $cm^{-1}$, 532 $cm^{-1}$, 458 $cm^{-1}$ for Ni(II) and Cu(II) complexes, respectively, were assigned to ν(M-O) and ν(M-N), validating the proposed coordination site of the ligand. Water vibrational bands were absent in both spectra, indicating that it was not present in the complex structure. This conclusion was further reinforced by the results of the CHN analysis. Therefore, it was determined that ligand (HBH-ANQ) functioned as a bianionic hexadentate ligand, binding to Ni(II) and Cu(II) ions through its enolic-O, azomethine-N and phenolic-O atoms [32,45,46].

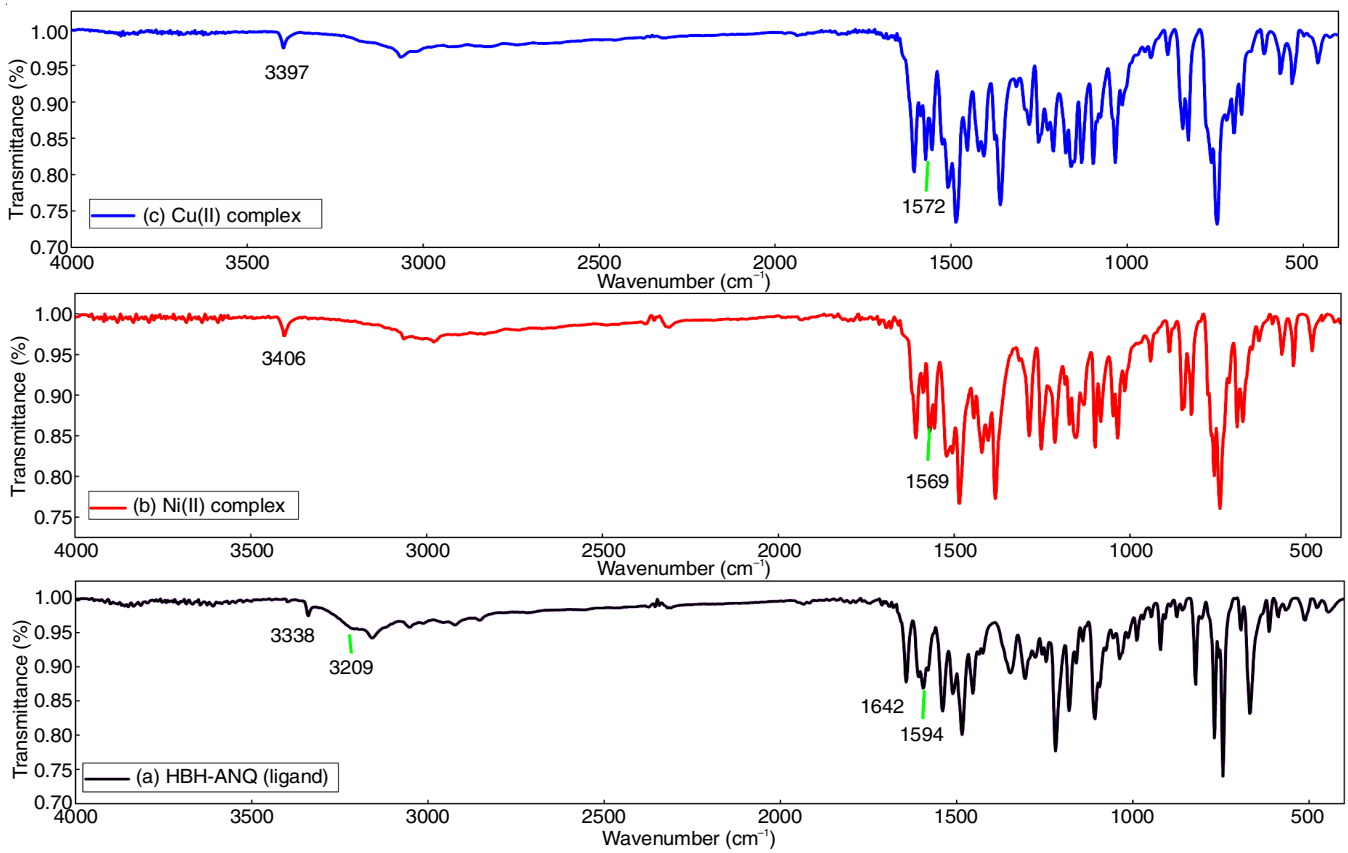


Fig. 2. FT-IR spectrum of (a) Schiff base ligand; (b) Ni(II) complex and (c) Cu(II) complex

In Co(II) and Zn(II) complexes IR spectrum, ν(N-H) and amide carbonyl stretching vibrational bands were observed at 3215-1643 $cm^{-1}$ and 3209-1643 $cm^{-1}$, respectively. The position of these bands is not changed indicating that none of these groups was involved in the complex formation as well as the ligand exists in the keto form in the complexes. The ν(C=N) band of the free ligand is moved to lower wavenumber, 1568 $cm^{-1}$ and 1566 $cm^{-1}$, respectively in the Co(II) and Zn(II) complexes, implying that the azomethine group through N-atoms coordinated with the metal ion. This was further confirmed by a red shift of the ν(N-N) stretching vibration band from 1108 $cm^{-1}$ to 1120 and 1118 $cm^{-1}$, respectively. The absence of a phenolic (O-H) stretching band and the appearance of the band at 1258 $cm^{-1}$ [Co(II)] and 1262 $cm^{-1}$ [Zn(II)] due to the phenolic (C-O) stretching, clearly indicate (O-H) groups have deprotonated and that phenolic-O atoms are participating in coordination. The absorption bands at 572 $cm^{-1}$, 483 $cm^{-1}$ and 561 $cm^{-1}$, 480 $cm^{-1}$ were attributed to ν(M-O) and ν(M-N), respectively. Thus, it is suggested that the Schiff base functioned as a bianionic tetradentate ligand in these complexes [4,47].

**UV-visible studies:** A DMSO solution containing $10^{-5}$ M of Schiff base ligand (HBH-ANQ) and its transition metal(II) chelates was used to measure their electronic spectra in the 200-1100 nm range (Fig. 3). Several absorption bands, ranging from 200 to 300 nm, could be attributed to the π→π* transitions of acenaphthacene and phenyl rings; these bands are almost entirely unaffected by complexation. On the other hand, the bands ranging from 310 to 420 nm, could be attributed to the n→π* transitions of the (O-H), (N-H), azomethine and carbonyl moieties; these bands were moved to longer wavelengths in metal complexes, indicating that they were involved in complex formation.

There is multiple absorption in the visible area of Co(II) complex spectrum. An absorption band observed at 710 nm can be assigned to the $^4A_2 \rightarrow {}^4T_1(P)$ transition, corresponding to the typical high spin tetrahedral environment and further supported by the measured magnetic moment values of 4.74 B.M. The nickel(II) complex exhibited three absorption bands in its electronic spectrum: 988 nm (10120 $cm^{-1}$), 535 nm (18691 $cm^{-1}$) and 463 nm (21598 $cm^{-1}$) that can be attributed to the $^3A_{2g} \rightarrow {}^3T_{2g}$ (F), $^3A_{2g} \rightarrow {}^3T_{1g}$ (F) and $^3A_{2g} \rightarrow {}^3T_{1g}$ (P) transitions, respectively, which are characteristic for the octahedral Ni(II) geometry. The $\nu_2/\nu_1$ ratio for the Ni(II) complex is lower than the typical range, indicating the presence of a distorted octahedral structure. The measured magnetic moment is 2.92 B.M. support the octahedral geometry. In $d^9$ configuration of Cu(II) complex, two bands were detected at 428 nm (23364 $cm^{-1}$) and 488 nm (20492 $cm^{-1}$), which correspond to the charge transfer and $^2E_g \rightarrow {}^2T_{2g}$ transition, respectively. The John-Teller effect causes peak broadening (470-554 nm), which indicates a distorted octahedral environment surrounding the Cu(II) ion. Further, this was supported by the observed magnetic moment (1.88 B.M.) of this complex. The electronic spectra of Zn(II) complex displayed an additional band at 438 nm, which can be attributed to ligand to metal charge transfer (LMCT). This complex was determined to be diamagnetic as a result of its $d^{10}$ configuration

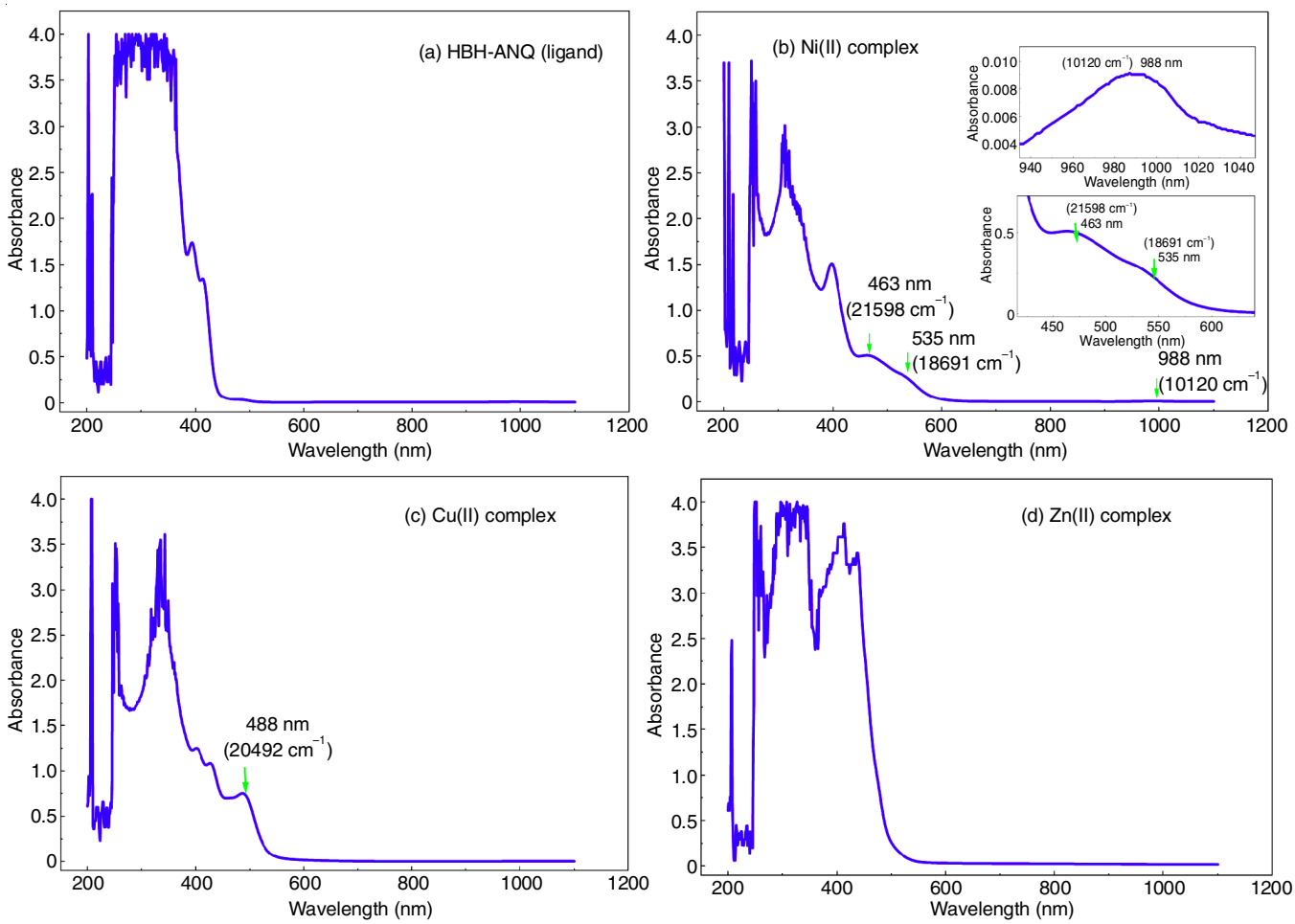


Fig. 3. UV-VIS spectrum of (a) Schiff base ligand; (b) Ni(II) complex; (c) Cu(II) complex and (d) Zn(II) complex

and did not display any *d-d* transitions. A tetrahedral geometry may be present in the Zn(II) complex, according to analytical and spectroscopic evidence [10,48,49].

**Thermal analysis:** Thermal investigations of Schiff base ligand and its metal(II) complexes was conducted to determine presence of the coordinated or lattice water molecules. The measurements of weight loss were made between 50 ºC and 800 ºC. The thermal behaviour of Schiff base ligand and its metal(II) complexes was examined using both TGA and DSC in nitrogen atmosphere (20 mL/min) at a heating rate of 20 ºC/min. The obtained thermal data are summarized in Table-3. The TG curve of free ligand (HBH-ANQ) shows three decomposition steps between the temperatures of 305-360 ºC, 360-460 ºC and 460-800 ºC. In the first step, a mass loss of 50.429% (calcd. 50.66%) is observed with DrTGA $T_{max}$ = 335 ºC and DSC peaks at 330 ºC (endothermic) and 335 ºC (exothermic) caused by the loss of phenolate [$C_6H_5O$] and [$C_7H_4NO_2$] moieties from Schiff base ligand. The following degradation may be related to the loss of [$C_4HN_3O$] fragment, since it resulted in a weight loss of 23.766% (calcd. 23.76%) with DrTGA maxima at 405 ºC. The final slow decomposition with mass loss of 5.4% (calcd. 5.33%) may attributed to loss of $C_2$ moiety, leading to formation of [$C_7H_8$] with the residual mass, 20.40% (calcd. 20.45%).

The thermogram curve of [Ni(HBH-ANQ)] indicates that the complex is thermally stable up to 365 ºC, after which the partial breakdown of the complex starts. It also reveals two stages of decomposition. The rapid first step decomposition with mass loss of 33.30% (calcd.33.36%) is observed between 365 ºC and 480 ºC with DrTGA maxima at 395 ºC, which can be ascribed to the loss of [$C_6H_4$] and phenolate [$C_6H_5O$] organic moieties from ligand backbone of the metal(II) complex, further reinforced by an endothermic maxima at 390 ºC and two exothermic peaks at 420 and 450 ºC on the DSC curve suggesting the decomposition of complex with melting. Up to 800 ºC, the final mass reduction of 15.083% (calcd. 16.57%) may have resulted from the elimination of 2[O=C=N-] parts, leaving residue [Ni($C_{12}H_7N_2O$)] with a mass of 51.617% (calcd. 50.10%), suggesting that complete ligand pyrolysis was not achieved [5,43].

In the TG curve of [Cu(HBH-ANQ)] complex, a mass loss of 3.751% in the range of 100-330 ºC was determined as the loss of adsorbed water or solvent molecule. It is possible that either moisture or solvent molecule was adsorbed onto the sample during handling or storage because the IR spectral and elemental analyses of the sample do not confirm this loss. Following a rapid degradation from 330 ºC to 415 ºC (DrTGA maxima at 370 ºC) with a DSC exothermic peak at 390 ºC, there was a weight loss of 36.734% (calcd. 36.37%) as a result of the loss of two weakly bonded phenolate [$C_6H_5O$] moieties from the ligand backbone of the complex. The final stage of

TABLE-3
THERMAL STUDIES DATA OF LIGAND AND ITS Co(II), Ni(II), Cu(II) AND Zn(II) COMPLEXES

| Compd. | n | TG | | Mass loss (%) Found (calcd.) | TGA decomposition assignment | DSC $T_{Peak}$ (°C) | Residue found (%) |
|---|---|---|---|---|---|---|---|
| | | Decomp. temp. range (°C) | DrTGA $T_{Peak}$ (°C) | | | | |
| **1** | 1 | 305-360 | 335 | 50.429 (50.66) | Loss of $[C_6H_5O]$ and $[C_7H_4NO_2]$ | 330, 335 | 20.405 |
| | 2 | 360-460 | 405 | 23.766 (23.76) | Loss of $[C_4HN_3O]$ | – | |
| | 3 | 460-800 | – | 5.4 (5.33) | Loss of $C_2$ | – | |
| **2** | 1 | 365-480 | 395 | 33.30 (33.36) | Loss of $[C_6H_4]$ and $[C_6H_5O]$ | 390, 420, 450 | 51.617 |
| | 2 | 480-800 | – | 15.083 (16.57) | Loss of 2[O=C=N-] | – | |
| **3** | 1 | 300-360 | 325 | 47.03 (46.36) | Loss of $[C_{13}H_7N_4O]$ | 320, 330 | 24.912 |
| | 2 | 360-485 | 420 | 23.67 (23.67) | Loss of $[C_7H_4O_2]$ | – | |
| | 3 | 485-800 | – | 4.388 (5.72) | Loss of $[C_2H_5]$ | – | |
| **4** | 1 | 100-330 | – | 3.751 | Loss of adsorbed moisture/solvent | – | 44.299 |
| | 2 | 330-415 | 370 | 36.73 (36.37) | Loss of 2$[C_6H_5O]$ | 370, 390 | |
| | 3 | 415-800 | – | 15.216 (16.40) | Loss of 2[O=C=N-] | 650 | |
| **5** | 1 | 300-355 | 325 | 45.895 (45.78) | Loss of $[C_{13}H_7N_4O]$ | 320, 330 | 29.175 |
| | 2 | 355-460 | 410 | 20.001 (20.07) | Loss of $[C_7H_3O]$ | 435 | |
| | 3 | 460-800 | – | 4.929 (4.29) | Loss of $H_2O$ and $2H_2$ | – | |

**1** = Ligand (HBH-ANQ); **2** = [Ni(HBH-ANQ)]; **3** = [Co(HBH-ANQ)]; **4** = [Cu(HBH-ANQ)]; **5** = [Zn(HBH-ANQ)]; n = number of decomposition steps.

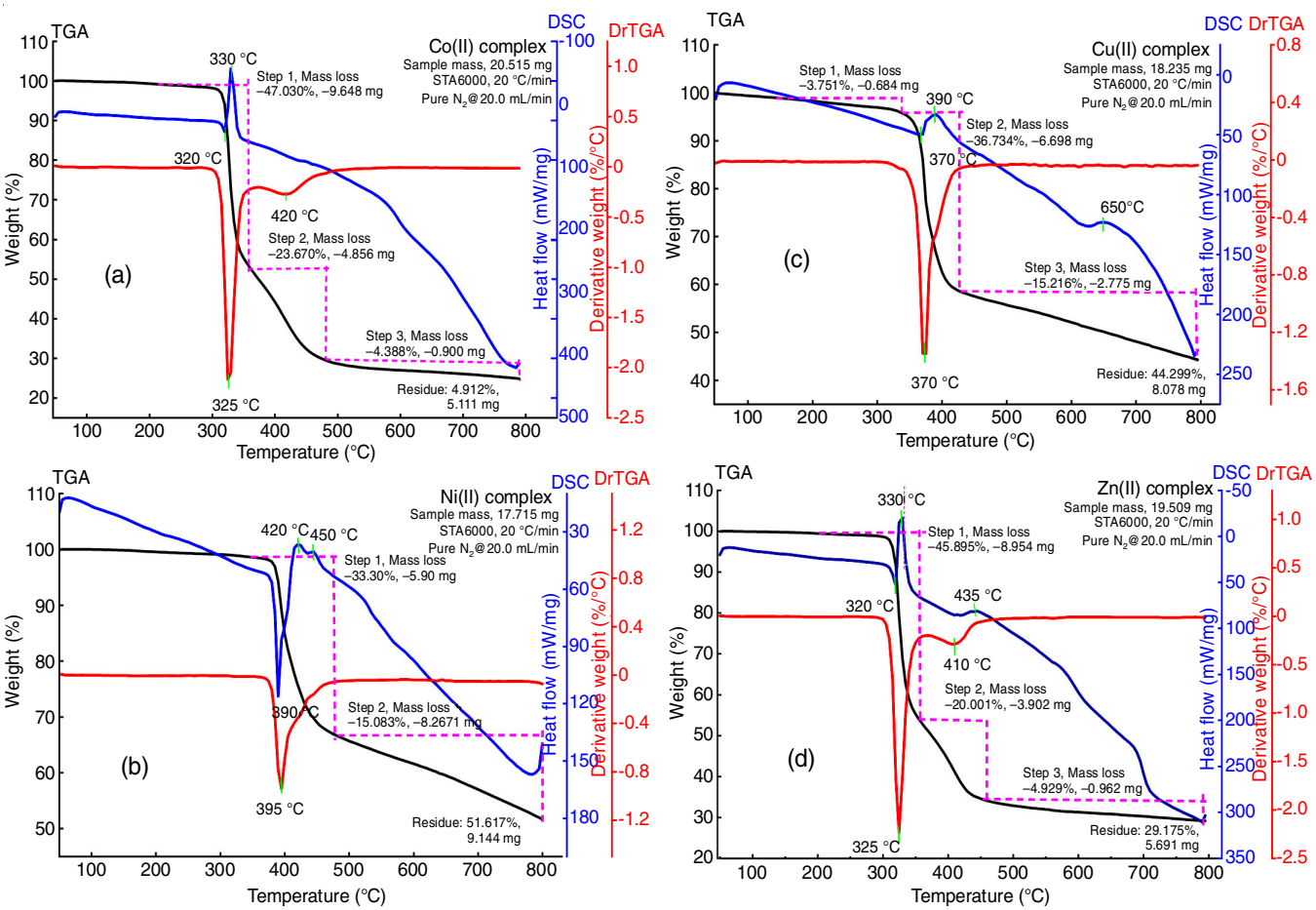


Fig. 4. Thermogram of (a) Co(II) complex; (b) Ni(II) complex; (c) Cu(II) complex and (d) Zn(II) complex

breakdown occurred gradually from 415 to 800 ºC with a weight loss of 15.216% (calcd. 16.40%). This was due to the elimination of 2[O=C=N-] fragments through an exothermic process that caused a broad peak ($T_{max}$ = 650 ºC) on the DSC curve. Up to 800 ºC, the Cu(II) complex does not completely decompose, leaving 44.30% of residual mass [47].

Three decomposition phases can be seen in the TG curve of [Co(HBH-ANQ)] complex. The Co(II) complex was stable up to 300 ºC, which indicates the absence of lattice/coordinated water molecules in a complex environment. The first step exhibits a rapid mass loss of 47.03% (calcd. 46.36%) in the temperature range of 300-360 ºC with DrTGA peak at 325 ºC and

DSC peaks at 320 ºC (endothermic) and 330 ºC (exothermic), which corresponds to the major loss of $[C_{13}H_7N_4O]$ portion of the organic ligand of complex. Due to the loss of $[C_7H_4O_2]$ organic moiety, a DrTGA maximum at 420 ºC was seen in the second breakdown step (360-485 ºC), resulting in a mass loss of 23.67% (calcd. 23.67%). The final phase of weight loss in the 485-800 ºC temperature range can be assigned to the full decomposition of the remaining organic portion of the complex, which accounts for 4.388% (calcd. 5.72%), leaving a residue of CoO + 4C with a mass of 24.19% (calcd. 24.25%).

The thermogram curve of the [Zn(HBH-ANQ)] complex comprises three degradation stages. No lattice or coordinated water molecule was found in a complex structure, as evidenced by the stability of the Zn(II) complex up to 300 ºC. The first step displays a significant drop in a mass of 45.89% (calcd. 45.78%) in the temperature range 300-355 ºC and precisely at 325 ºC (DrTGA), corresponding to the loss of $[C_{13}H_7N_4O]$ with the appearance of an endothermic and an exothermic peak at 320 ºC and 330 ºC on the DSC curve, respectively indicating decomposition with the melting of the complex. In the next decomposition step (355-460 ºC), the lost mass of 20.001% (calcd. 20.07%) with DrTGA maxima at 410 ºC observed due to loss of $[C_7H_3O]$ moiety which caused DSC peak at 435 ºC. In the final stage (460-800 ºC), the slow weight loss of 4.929.6% (calcd. 4.29%) was observed due to the removal of $H_2O$ and $2H_2$ by complete degradation of the remaining organic moiety, leading to the formation of stable ZnO which was contamination with carbon residue having a mass of 29.17% (calcd. 29.86%) [9,16].

**Powder XRD studies:** It was found that all compounds exhibit a high degree of crystallinity, by studying the diffractograms that were obtained. Fig. 5 displays the powder XRD pattern of Schiff base ligand (HBH-ANQ) and its Co(II), Ni(II), Cu(II) and Zn(II) complexes. For instance, diffractogram of the nickel(II) complex registered 8 reflection peaks in the range of (2θ) 5 to 50º with maxima at 2θ = 8.70º with a corresponding d spacing value of 10.156 Å where the significant crystalline peaks of the Ni(II) complex are observed at 2θ = 6.12º, 8.70º, 9.74º, 12.36º, 13.84º, 18.10º, 22.02º and 26.60º.

Furthermore, the diffractogram of the Schiff base ligand, Co(II), Cu(II) and Zn(II) complexes contained 11, 6, 6 and 5 significant reflection peaks in the range of (2θ) 5º to 50º with maxima at 2θ = 6.32º, 14.86º, 8.64º and 14.84º, which corresponded to d spacing values of 13.974 Å, 5.957 Å,10.226 Å and 5.965 Å, respectively. The size of the crystallite was determined by analyzing the XRD patterns and measuring the full width at half maximum (FWHM) of the prominent intensity peaks. This was done using Debye Scherrer's equation, $D = K\lambda/\beta\cos\theta$, where K is a constant with a value of 0.94 for a Cu grid, λ is the X-ray wavelength with a value of 1.5406 Å, θ is the Bragg diffraction angle, D represents the particle size of the crystal grain and β stands for the FWHM of the characteristic Bragg reflection peak. The crystallite sizes were found in the range of (11.31-23.12 nm), (17.12-21.48 nm), (18.06-20.48 nm), (16.49-18.58 nm) and (11.52-18.53 nm) for Schiff base ligand, Co(II), Ni(II), Cu(II) and Zn(II) complexes, giving an average crystallite size of 18.01 nm, 18.55 nm, 18.78 nm, 17.94 nm and 16.83 nm, respectively. The distribution of lattice constants resulting from crystal imperfections was measured by the lattice strain (ε), which can be ascribed to defects and dislocations at the grain boundaries. The relation $\varepsilon = \beta/4\tan\theta$, was used to evaluate lattice strain [50] and the lattice strain (ε) value was found in the range of (6.73 to 35.32 × $10^{-3}$ nm), (6.98 to 31.44 × $10^{-3}$ nm), (8.25 to 36.48 × $10^{-3}$ nm), (8.27 to 36.72 × $10^{-3}$ nm) and (8.03 to 31.44 × $10^{-3}$ nm) with giving an average lattice strain value of 15.39 × $10^{-3}$, 15.98 × $10^{-3}$, 18.43 × $10^{-3}$, 20.77 × $10^{-3}$ and 18.97 × $10^{-3}$ nm for the Schiff base ligand (HBH-ANQ), Co(II), Ni(II), Cu(II) and Zn(II) complexes, respectively. Additionally, the number of dislocations in a unit volume of a crystalline material is measured by the dislocation density (δ), which was calculated using Williamson & Smallman's relation, $\delta = 1/D^2$ [51] and the range of dislocation density was shown to be between (1.87 -5.31 × $10^{-3}$ $nm^{-2}$), (2.16-3.41 × $10^{-3}$ $nm^{-2}$), (2.38-3.06 × $10^{-3}$ $nm^{-2}$), (2.89-3.68 × $10^{-3}$ $nm^{-2}$) and (3.04-7.54 × $10^{-3}$ $nm^{-2}$) with an average dislocation density value of 3.51 × $10^{-3}$, 2.95 × $10^{-3}$, 2.85 × $10^{-3}$, 3.12 × $10^{-3}$ and 3.94 × $10^{-3}$ $nm^{-2}$ for the free ligand, Co(II), Ni(II), Cu(II) and Zn(II) complexes, respectively [35].

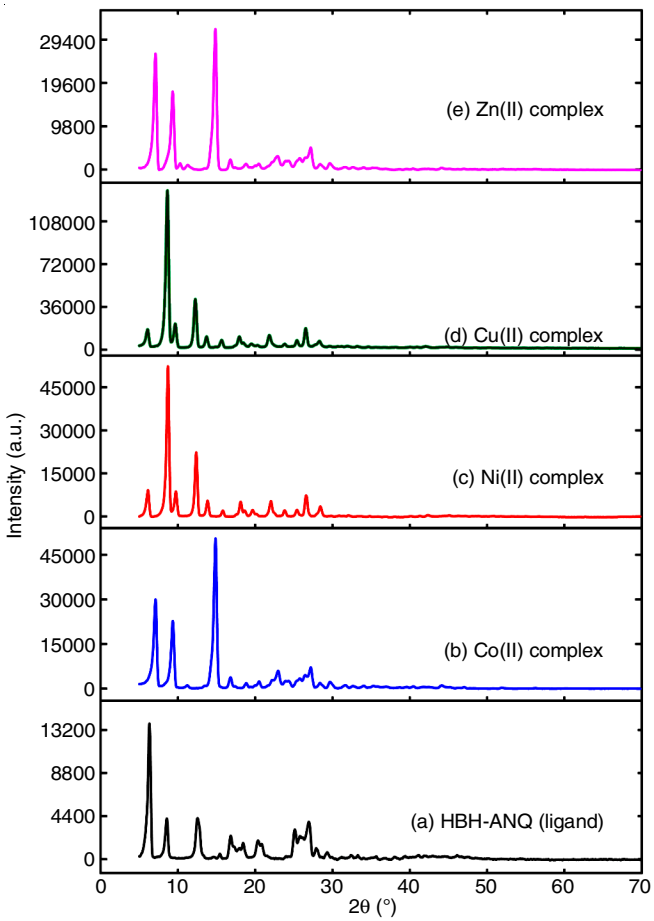


Fig. 5. Powder X-ray diffraction pattern of (a) Schiff base ligand (HBH-ANQ); (b) Co(II) complex; (c) Ni(II) complex; (d) Cu(II) complex and (e) Zn(II) complex

***In vitro* antioxidant studies:** The antioxidant activity of the synthesized compounds at various doses using the DPPH free radical was evaluated. The scavenging activity of the com-

pounds was observed to exhibit a positive correlation with the concentration. Free Schiff base scavenged 29% of DPPH radicals at low concentration and 40% at high concentration; however, its effectiveness was significantly increased upon complexation with metal ions. The Cu(II) complex was the most active compound, demonstrating the highest level of scavenging activity at both low and high concentrations, with scavenging activities of 49% and 68%, respectively, while Zn(II) complex exhibited the lowest level of scavenging activity, ranging from 32% to 42% for low to high concentrations. The compounds that were evaluated including the standard were found to exhibit DPPH radical scavenging activities in the following order: ascorbic acid > Cu(II) complex > Ni(II) complex > Co(II) complex > Zn(II) complex > Schiff base ligand. The conclusion was that metal ions in the complexes may have an electron-withdrawing effect that facilitates the release of electrons or hydrogen radicals and scavenge the DPPH radical [35].

***In vitro* antimicrobial studies:** The disc diffusion method was utilized with an agar medium to assess the antibacterial and antifungal potentials of synthesized Schiff base ligand and its metal(II) complexes against bacteria *viz*. *Corynebacterium*, *Staphylococcus aureus*, *Bacillus subtilis*, *Pseudomonas aeruginosa*, *Klebsiella pneumoniae*, *Escherichia coli* and fungi *viz*. *Aspergillus niger*, *Aspergillus flavus* and *Candida albicans*, respectively. All the compounds were examined for their antimicrobial activities with doses of 50 µg/disc and 100 µg/disc, as shown in Figs. 6 and 7, respectively. The Schiff base and its metal(II) complexes displayed different levels of growth inhibition in the bacterial and fungal species being studied. The antibacterial study of the investigated substances revealed that the Cu(II) and Ni(II) complexes exhibited excellent antibacterial activity against both Gram-positive and Gram-negative bacteria, but the Co(II) and Zn(II) complexes demonstrated relatively lower levels of antibacterial activity, except all metal(II) complexes effectively inhibiting the growth of *Corynebacterium*. The Schiff base ligand was ineffective against *K. pneumoniae* and *E. coli* and less active against *B. subtilis* and *P. aeruginosa*, but had considerable effectiveness against *S. aureus* and *Corynebacterium*. The general order of the antibacterial activity of the synthesized compounds against Gram-positive bacteria is as follows: Cu(II) = Ni(II) > Co(II) = Zn(II) > L, while against Gram-negative bacteria it is Cu(II) > Co(II) = Ni(II) > Zn(II) = L, respectively. According to an antifungal study, the Co(II) complex has a higher antifungal activity against *C. albicans*, *A. niger* and *A. flavus*, while the Ni(II), Cu(II) and Zn(II) complexes have a lower antifungal activity. On the other hand, the ligand did not affect the growth of fungi. In general, chelated Schiff base compounds exhibit greater antimicrobial potential than corresponding unchelated Schiff base under identical experimental conditions. The chelation theory explains the enhanced activity exhibited by metal chelates. Chelation reduces metal ion polarity by partially sharing its positive charge with ligand donor groups and delocalizing electrons over the chelate ring. This makes the metal chelate more lipophilic, allowing it to enter microbe membrane lipid layers and kill them. Ligand-metal ion interactions can also change system, solubility, dipole moment and conductivity, affecting antibacterial potential [10,52].

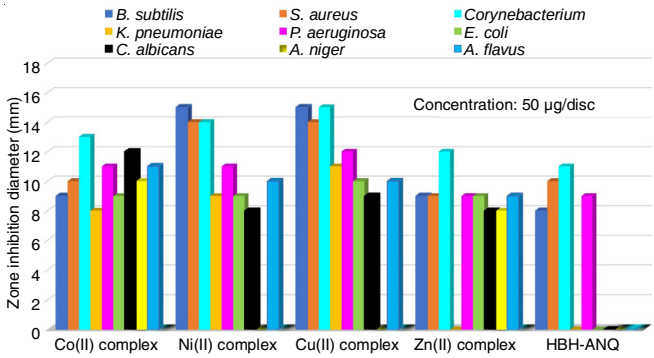


Fig. 6. Antibacterial and antifungal activities of ligand and its metal complexes at 50 µg concentration

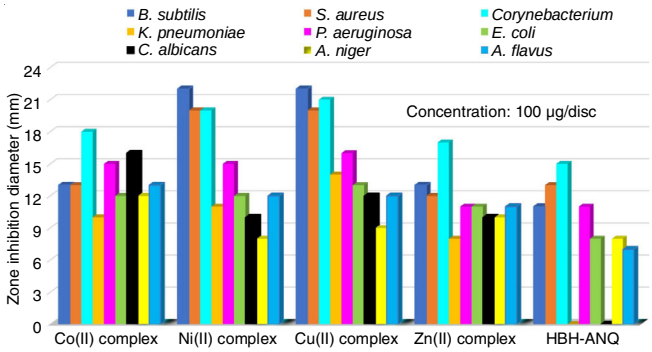


Fig. 7. Antibacterial and antifungal activities of ligand and its metal complexes at 100 µg concentration

## Conclusion

The newly synthesized Schiff base (HBH-ANQ) and its metal(II) complexes were characterized by various physical, spectroscopic and analytical techniques. It was found that the metal to ligand ratio was 1:1 in all the metal(II) complexes. The Schiff base functioned as a bianionic hexadentate ligand, binding metal ions through its enolic-O, azomethine-N and phenolic-O atoms, providing an octahedral geometry for the Ni(II) and Cu(II) complexes, whereas it functioned as a bianionic tetradentate ligand, binding metal ions *via* azomethine-N and phenolate-O atoms, forming tetrahedral Co(II) and Zn(II) complexes. The thermal studies showed that the all metal(II) complexes did not contain coordinated or lattice water molecules and all of them showed good thermal stability. All compounds are well-crystallized and the estimated average particle size is in the nanoscale region, according to powder XRD data. The DPPH assays revealed that the metal(II) complexes exhibit greater efficacy as antioxidants and scavengers of free radicals compared to the Schiff base. Antimicrobial activity against bacteria and fungi was assessed *in vitro* using the disc diffusion technique for all substances. This study found that compared to Schiff base ligand, metal(II) complexes exhibited much higher inhibitory action. The most efficient inhibitors of bacteria were Cu(II) and Ni(II) complexes, while all fungi were well inhibited by Co(II) complex.

## ACKNOWLEDGEMENTS

The authors would like to extend their sincere appreciation to the Department of Chemistry, Changu Kana Thakur Arts,

Commerce & Science College, New Panvel, Mumbai, India for providing the research facilities.

## CONFLICT OF INTEREST

The authors declare that there is no conflict of interests regarding the publication of this article.

## REFERENCES


1. C. Boulechfar, H. Ferkous, A. Delimi, A. Djedouani, A. Kahlouche, A. Boublia, A.S. Darwish, T. Lemaoui, R. Verma and Y. Benguerba, *Inorg. Chem. Commun.*, **150**, 110451 (2023); https://doi.org/10.1016/j.inoche.2023.110451
2. A. Subashini, P. Priyadharsani, K. Thamaraiselvi, V. Veeramani, P. Rose, R. Philip, H. Stoeckli-Evans, K. Ramamurthi and R.R. Babu, *J. Mater. Sci. Mater. Electron.*, **30**, 2638 (2019); https://doi.org/10.1007/s10854-018-0539-2
3. A.-A.B.O. Ali, A.J.M. Al-Karawi, N. Dege, S. Kansiz and H.A.D. Ithawi, *J. Mol. Struct.*, **1217**, 128387 (2020); https://doi.org/10.1016/j.molstruc.2020.128387
4. S.A. Aboafia, S.A. Elsayed, A.K.A. El-Sayed and A.M. El-Hendawy, *J. Mol. Struct.*, **1158**, 39 (2018); https://doi.org/10.1016/j.molstruc.2018.01.008
5. I. Al-Qadsy, A.-B. Al-Odayni, W.S. Saeed, A. Alrabie, A. Al-Adhreai, L.A.S. Al-Faqeeh, P. Lama, A.A. Alghamdi and M. Farooqui, *Crystals*, **11**, 110 (2021); https://doi.org/10.3390/cryst11020110
6. E. Raczuk, B. Dmochowska, J. Samaszko-Fiertek and J. Madaj, *Molecules*, **27**, 787 (2022); https://doi.org/10.3390/molecules27030787
7. A.-A.B. OmarAli, A.J.M. Al-Karawi, A.A. Awad, N. Dege, S. Kansiz, E. Agar, Z.A. Hussein and I.R. Mohammed, *Acta Crystallogr. C Struct. Chem.*, **76**, 476 (2020); https://doi.org/10.1107/S2053229620004994
8. K. Ananthi, H. Anandalakshmi, A. Nepolraj and S. Akshaya, *Substantia*, **8**, 25 (2024); https://doi.org/10.36253/Substantia-2294
9. D.A. Tolan, T.I. Kashar, K. Yoshizawa and A.M. El-Nahas, *Appl. Organomet. Chem.*, **35**, e6205 (2021); https://doi.org/10.1002/aoc.6205
10. M. Yadav, S. Sharma and J. Devi, *J. Chem. Sci.*, **133**, 21 (2021); https://doi.org/10.1007/s12039-020-01854-6
11. P. Tyagi, S. Chandra and B. Saraswat, *Spectrochim. Acta A Mol. Biomol. Spectrosc.*, **134**, 200 (2015); https://doi.org/10.1016/j.saa.2014.06.112
12. A A R. Despaigne, G.L. Parrilha, J.B. Izidoro, P.R. da Costa, R.G. dos Santos, O.E. Piro, E.E. Castellano, W.R. Rocha and H. Beraldo, *Eur. J. Med. Chem.*, **50**, 163 (2012); https://doi.org/10.1016/j.ejmech.2012.01.051
13. R. Mohareb, K. El-Sharkawy, M. Hussein and H. El-Sehrawi, *J. Pharm. Sci. Res.*, **2**, 185 (2010).
14. W.B. Júnior, M.S. Alexandre-Moreira, M.A. Alves, A. Perez-Rebolledo, G.L. Parrilha, E.E. Castellano, O.E. Piro, E.J. Barreiro, L.M. Lima and H. Beraldo, *Molecules*, **16**, 6902 (2011); https://doi.org/10.3390/molecules16086902
15. U. Salgin-Göksen, N. Gökhan-Kelekçi, Ö. Göktas, Y. Köysal, E. Kiliç, S. Isik, G. Aktay and M. Özalp, *Bioorg. Med. Chem.*, **15**, 5738 (2007); https://doi.org/10.1016/j.bmc.2007.06.006
16. O.K. Olurotimi, A.J. Adeyemi, B.O. Agbeke, O. Olajumoke, S.T. Oluwasegun and E.G. Sunday, *Orient. J. Chem.*, **33**, 1623 (2017); https://doi.org/10.13005/ojc/330405
17. W.M. Eldehna, M. Fares, M.M. Abdel-Aziz and H.A. Abdel-Aziz, *Molecules*, **20**, 8800 (2015); https://doi.org/10.3390/molecules20058800
18. J.R. Dimmock, S.C. Vashishtha and J.P. Stables, *Eur. J. Med. Chem.*, **35**, 241 (2000); https://doi.org/10.1016/S0223-5234(00)00123-9
19. P. Melnyk, V. Leroux, C. Sergheraert and P. Grellier, *Bioorg. Med. Chem. Lett.*, **16**, 31 (2006); https://doi.org/10.1016/j.bmcl.2005.09.058
20. S.V. Bhandari, K.G. Bothara, A.A. Patil, T.S. Chitre, A.P. Sarkate, S.T. Gore, S.C. Dangre and C.V. Khachane, *Bioorg. Med. Chem.*, **17**, 390 (2009); https://doi.org/10.1016/j.bmc.2008.10.032
21. M. Mishra, K. Tiwari, S. Shukla, R. Mishra and V.P. Singh, *Spectrochim. Acta A Mol. Biomol. Spectrosc.*, **132**, 452 (2014); https://doi.org/10.1016/j.saa.2014.05.007
22. P.P. Netalkar, A. Kamath, S.P. Netalkar and V.K. Revankar, *Spectrochim. Acta A Mol. Biomol. Spectrosc.*, **97**, 762 (2012); https://doi.org/10.1016/j.saa.2012.07.066
23. A. Sundar, M. Prabhu, N. Indra Gandhi, M. Marappan and G. Rajagopal, *Spectrochim. Acta A Mol. Biomol. Spectrosc.*, **129**, 509 (2014); https://doi.org/10.1016/j.saa.2014.03.084
24. T. Mistri, M. Dolai, D. Chakraborty, A.R. Khuda-Bukhsh, K.K. Das and M. Ali, *Org. Biomol. Chem.*, **10**, 2380 (2012); https://doi.org/10.1039/c2ob07084g
25. J. Devi, S. Devi and A. Kumar, *MedChemComm*, **7**, 932 (2016); https://doi.org/10.1039/C5MD00554J
26. M. Jain, S. Maanju and R.V. Singh, *Appl. Organomet. Chem.*, **18**, 471 (2004); https://doi.org/10.1002/aoc.711
27. M. Chinnasamy and A. Ramu, *Asian J. Chem.*, **31**, 2941 (2019); https://doi.org/10.14233/ajchem.2019.22308
28. P.A. Fatullayeva, *J. Chemical Problems*, **19**, 79 (2021); https://doi.org/10.32737/2221-8688-2021-2-79-83
29. E.S.H. ElAshry, H.A. Hamid, A.A. Kassem and M. Shoukry, *Molecules*, **7**, 155 (2002); https://doi.org/10.3390/70200155
30. Z. Zhang, H. Yang, G. Wu, Z. Li, T. Song and X.Q. Li, *Eur. J. Med. Chem.*, **46**, 3909 (2011); https://doi.org/10.1016/j.ejmech.2011.05.062
31. Y.S. El-Alawi, B.J. McConkey, D. George Dixon and B.M. Greenberg, *Ecotoxicol. Environ. Saf.*, **51**, 12 (2002); https://doi.org/10.1006/eesa.2001.2108
32. M. Kumar, S. Roy, M.S.H. Faizi, S. Kumar, M.K. Singh, S. Kishor, S.C. Peter and R.P. John, *J. Mol. Struct.*, **1128**, 195 (2017); https://doi.org/10.1016/j.molstruc.2016.08.004
33. R.B. Bennie, S.T. David, C. Joel, S.D. Abraham and S.I. Pillai, *Int. J. Inorg. Bioinorg. Chem.*, **5**, 49 (2015).
34. S.M. Sathyasheeli, S.T. David, C.V. Mythili and P.S. Suja Pon Mini, *Der Pharma Chem.*, **8**, 312 (2016).
35. T.S. Umasare and S.K. Patil, *Asian J. Chem.*, **35**, 1932 (2023); https://doi.org/10.14233/ajchem.2023.28058
36. S. Kumar, A. Hansda, A. Chandra, A. Kumar, M. Sithambaresan, M.S.H. Faizi, M. Kumar, V. Kumar and R.P. John, *Polyhedron*, **134**, 11 (2017); https://doi.org/10.1016/j.poly.2017.05.055
37. U. El-Ayaan and A.A. Abdel-Aziz, *Eur. J. Med. Chem.*, **40**, 1214 (2005); https://doi.org/10.1016/j.ejmech.2005.06.009
38. S.R. Pattan, P.A. Rabara, J.S. Pattan, A.A. Bukitagar, V.S. Wakale and D.S. Musmade, *Indian J. Chem.*, **48B**, 1453 (2009).
39. I.P. Ejidike and P.A. Ajibade, *Molecules*, **20**, 9788 (2015); https://doi.org/10.3390/molecules20069788
40. M. Yadav, S. Sharma and J. Devi, *J. Chem. Sci.*, **133**, 21 (2021); https://doi.org/10.1007/s12039-020-01854-6
41. M. Balouiri, M. Sadiki and S.K. Ibnsouda, *J. Pharm. Anal.*, **6**, 71 (2016); https://doi.org/10.1016/j.jpha.2015.11.005
42. M.A. Rizk, M.A. Alsaiari, R.A. Alsaiari, I.A. Ibrahim, A.M. Abbas and G.M. Khairy, *Chemosensors*, **11**, 570 (2023); https://doi.org/10.3390/chemosensors11120570
43. R.R. Zaky, K.M. Ibrahim and I.M. Gabr, *Spectrochim. Acta A Mol. Biomol. Spectrosc.*, **81**, 28 (2011); https://doi.org/10.1016/j.saa.2011.05.028
44. A. Setyawati, T. D.Wahyuningsih and B. Purwono, *AIP Conf. Proc.*, **1823**, 020121 (2017); https://doi.org/10.1063/1.4978194
45. P. Joshi, S.R. Ali, V.K. Rishu and V.K. Bhardwaj, *Luminescence*, **36**, 986 (2021); https://doi.org/10.1002/bio.4025
46. T. Mangamamba, M.C. Ganorkar and G. Swarnabala, *Int. J. Inorg. Chem.*, **2014**, 736538 (2014); https://doi.org/10.1155/2014/736538

47. D.S. Badiger, R.S. Hunoor, B.R. Patil, R.S. Vadavi, C.V. Mangannavar, I.S. Muchchandi and K.B. Gudasi, *J. Mol. Struct.*, **1019**, 159 (2012); https://doi.org/10.1016/j.molstruc.2012.02.062
48. A.S. El-Tabl, M. Mohamed Abd El-Waheed, M.A. Wahba and N.A. El-Halim Abou El-Fadl, *Bioinorg. Chem. Appl.*, **2015**, 126023 (2015); https://doi.org/10.1155/2015/126023
49. C. Anitha, S. Sumathi, P. Tharmaraj and C.D. Sheela, *Int. J. Inorg. Chem.*, **2011**, 493942 (2011); https://doi.org/10.1155/2011/493942
50. P. Chelvanathan, Y. Yusoff, F. Haque, M. Akhtaruzzaman, M.M. Alam, Z.A. Alothman, M.J. Rashid, K. Sopian and N. Amin, *Appl. Surf. Sci.*, **334**, 138 (2015); https://doi.org/10.1016/j.apsusc.2014.08.155
51. M.A. Mahmud, N.K. Elumalai, M.B. Upama, D. Wang, F. Haque, C. Xu, M. Wright and A. Uddin, *Sol. Energy Mater. Sol. Cells*, **167**, 70 (2017); https://doi.org/10.1016/j.solmat.2017.03.032
52. M.O. Agwara, P.T. Ndifon, N.B. Ndosiri, A.G. Paboudam, D.M. Yufanyi and A. Mohamadou, *Bull. Chem. Soc. Ethiop.*, **24**, 383 (2010); https://doi.org/10.4314/bcse.v24i3.60680